



Clinical Neuroscience

An extension of olfactometry methods: An expandable, fully automated, mobile, MRI-compatible olfactometer



Anne-Kathrin Bestgen^{a,*¹}, Patrick Schulze^{a,b,1}, Lars Kuchinke^a, Boris Suchan^a, Thilo Derdak^a, Tobias Otto^a, Birger Jettkant^b, Kirsten Sucker^b

^a Department of Psychology, Ruhr-University Bochum, Universitätsstraße 150, 44801 Bochum, Germany

^b Institute for Prevention and Occupational Medicine of the German Social Accident Insurance (IPA), Institute of the Ruhr-University Bochum, Bürkle-de-la-Camp-Platz 1, 44789 Bochum, Germany

HIGHLIGHTS

- Presentation of an olfactometer design to overcome the challenges in fMRI experiments.
- Challenges due to the magnetic environment, space and experimental designs are addressed.
- Functional efficiency is confirmed by results of an fMRI study and a massspectrometer.
- Activation in piriform cortex, OFC, amygdala, insula and hippocampus.
- Stable odor concentration over time measured with CIMS.

ARTICLE INFO

Article history:

Received 15 October 2015

Received in revised form

16 December 2015

Accepted 17 December 2015

Available online 29 December 2015

Keywords:

Olfactometer

fMRI

Human olfaction

Odor quality

Olfactory cognition

ABSTRACT

Background: fMRI experiments on olfaction offer new insights into the complex, but in contrast to other sensory systems, less studied cognition of odors. To perform these experiments is still a challenge.

New method: To address the challenge posed by MR settings, an olfactometer design is presented including specific improvements to the limited number of already existing olfactometers. Innovative features such as pneumatically controlled pinch valves, useable in the scanner and providing exact stimulus timing as well as a 3D-printed nasal mask inlet for common sleep laboratory masks that can be used for lateral divided stimulus presentation are introduced. To ensure a fully automated and mobile system, the use of a flexible and easily-adapted Matlab-Code and a portable adaptable container system are presented.

Results: The functional efficiency of these features are proven by results of an fMRI study as well as testing temporal resolution and concentration stability with a mass spectrometer.

Comparison with existing methods: The 24-channel olfactometer design presented here provides an inexpensive alternative to the currently available olfactometers including the achievement of fast onset times, lateral divided stimulus presentation and high flexibility and adaptability to different scientific questions.

Conclusion: The olfactometer design presented in this paper can be seen as a realistic and feasible solution to overcome the challenges of presenting olfactory stimuli within the MR setting.

© 2015 Elsevier B.V. All rights reserved.

1. Introduction

Research in the field of neuroscience with a focus on olfaction is growing, but the accurate presentation of olfactory stimuli in the MR setting is still a challenge to the investigator. The reasons

for this are limitations and challenges posed by the (1) magnetic environment, (2) space and (3) experimental designs.

Here, we present an olfactometer design that addresses these issues with different extensions to the already existing olfactometers currently used for fMRI studies (Andrieu et al., 2014; Borromeo et al., 2010; Cuevas et al., 2010; Lorig et al., 1999; Lowen and Lukas, 2006; Popp et al., 2004; Sezille et al., 2013; Sobel et al., 1997; Sommer et al., 2012; Vigouroux et al., 2005).

The innovations can be added to a present olfactometer that fulfill the requirements of a basic construction plan of an olfactometer (e.g. Kobal and Hummel, 1988), or might be of importance

* Corresponding author at: Department of Psychology, Ruhr-University Bochum, Universitätsstraße 150, GAF 04/423, 44801 Bochum, Germany.

E-mail address: anne-kathrin.bestgen@rub.de (A.-K. Bestgen).

¹ These authors contributed equally to this manuscript.

to take into account at the beginning of the construction of a new olfactometer.

Specific features such as pneumatically controlled pinch valves that are useable in the scanner and provide exact stimulus timing as well as a 3D-printed nasal mask inlet for common sleep laboratory masks that can be used for lateral divided stimulus presentation are introduced in the material section. A well-conceived construction plan including a container system is presented to construct a mobile olfactometer adapted for MR settings. Furthermore, pneumatic and electric plans of the complete olfactometer as well as a complete material-list are provided. Moreover, the functional efficiency of these features are proven by results of a fMRI study and by testing the temporal resolution and concentration stability with a high performance, real time chemical ionization mass spectrometer (CIMS, Airsense.net, MS4 GmbH, Germany). These data are reported in the experimental validation section.

2. Materials

In this section the adapted components of the olfactometer are introduced as solutions for the existing challenges: (1) magnetic environment, (2) space and (3) experimental designs in fMRI studies.

2.1. The magnetic environment

In an fMRI study, participants lay in a strong magnetic field, which makes it impossible to use any magnetic or electric parts close to the participant. To address the problem of the strong magnetic field within the MR testing room, the here described olfactometer is split into two functional units: The control unit which contains the control components to select the different odors from the odor bottles, and the delivery unit which consists of all parts that support the interface between the olfactometer and the participant. Most parts of the delivery unit lay within the MR testing room and are customized to contain no metal or electrical parts. In studies on olfaction it is necessary to have valves close to the participants to ensure precise temporal stimulation for fast onset and offset times. Given the distance between the MR control room and the MR scanner, it is nearly impossible to achieve fast on- and offset times without additional valves close to the participant or with a high flow. For this purpose pneumatically controlled plastic pinch valves are custom built (Fig. 1). The advantage of using these plastic pinch valves is the possibility to fill the tubes from the odor bottles to these pinch valves prior to each odor presentation. Thus, only the small distance (15 cm) between the pinch valve and the participants' nose has to be overcome. For customization, the inlet of a proportional media valve (FESTO, Germany series: VZQA-series) is placed into a polyvinyl chloride (PVC) pressure pipe. The pressure pipe comprises a wall thickness of 10 mm and a maximum operating pressure of 16 bar. The pinch valve is a 2/2-way valve for controlling media flows, which is open in normal position. The inlet is a tubular pinch valve sleeve made from elastomer (ethylene

propylene diene monomer – EPDM). When pilot air is admitted, the tubular pinch valve sleeve closes which interrupts the media flow (as long as the pilot air is admitted). The cylindrical pinch valve is 10 cm long and has an outer diameter of 4 cm. No metal or electrical parts are used for this valve. Thus, interference with the MR setting is avoided while temporally precise stimulation is still possible. These valves also provide the use of independent channels for each odor, this way a cross contamination of odors is avoided.

To ensure that the valves are as close as possible to the participant, all valves are sewn into a blanket. With a weight of approximately 1.5 kg the blanket containing the valves has the advantage of being highly comfortable for the participants and, thus, replaces the standard blanket that is often offered to the participants because of the low temperatures in the MR scanner (Fig. 5). Twelve meter long tubings with an inner diameter of 3 mm connect the control unit and the delivery unit, which allows a storage of the control section in the control room of fMRI laboratories, without disadvantages for the airflow. Polyethylene, food-safe and chemical resistant tubings are chosen with a small diameter to be able to fit as many channels through the waveguides of the MR setting as possible.

2.2. Limitations of space

Our goal was to develop an olfactometer-design, which is flexible and thus adaptable to many different experimental needs and also to different experimental facilities. For a setup, which suits in many experimental environments two demands must be met: (1) The olfactometer needs to be as small as possible to fit into most laboratories and to take up as little space as possible for storage if not needed. (2) The olfactometer has to be mobile in a way that it can be moved between different laboratories.

(1) To minimize the size of the olfactometer, the focus lies in incorporating the smallest possible parts, for example instead of using many single solenoid valves miniature valve terminals are incorporated, which take up significantly less space (Fig. 2). A valve terminal for 24 valves is only 3.1 cm high, 3.5 cm wide and 33.2 cm long. An additional advantage of these terminals is the use of a single electrical multi-pin connector, which enables the use of only one cable to control all valves. This is additionally space saving and simplifies the setup and service of the olfactometer. Despite its compact design the valve terminals themselves have a fast response of 4 ms. Air monitoring apparatuses, such as pressure sensors and flowmeter, in digital forms, function as constant control systems with a good ratio in terms of space. For example the digital flowmeter is capable of reporting and controlling the air flow of multiple odor channels in parallel by sampling the acquired data directly into the software which controls the olfactometer. Thus, it enables the experimenter to get reports of airflow for each odor channel separately.

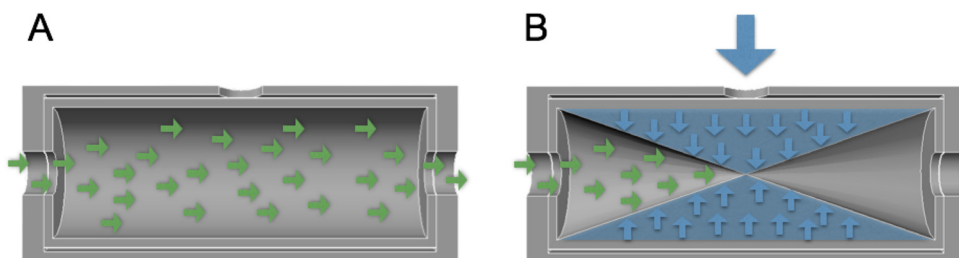


Fig. 1. Schematic illustration of a pneumatically controlled plastic pinch valve. (A) Opened pinch valve: odor can pass the valve and reach the participants nose. (B) Closed pinch valve. When pilot air is added to the valve, the inner pinch balloon is pressed together and the odor cannot reach the participants nose.

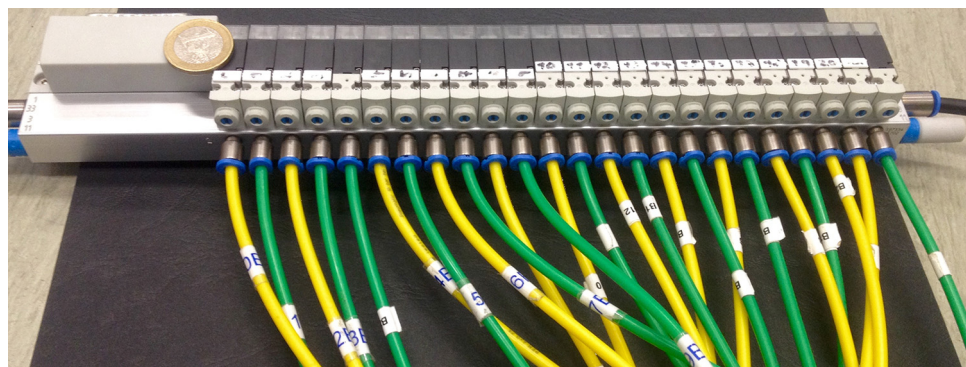


Fig. 2. Valve terminal with 24 valves connected to the tubes with an inner diameter of 3 mm. For illustration purposes an one euro coin ($d=23$ mm) is presented together with the terminal.

Moreover, the issue of the limited space between the participants face and the head coils in the MR scanner, can be solved by using a common sleep laboratory mask prepared with a 3D-printed nasal mask inlet (Fig. 3, the AutoCAD drawing can be found in [supplementary materials](#)). Additionally, due to the perfect fit under the head coil, this nosepiece enables the use of MRI LCD goggles despite the limited space within the head coils.

- (2) At the same time the olfactometer needs to be mobile to ensure an easy transportation. A container system with wheels, which is even expandable due to a lock-connection system, ensures easy transportation (Fig. 4). The container system used here consists of four separate containers (TANOS, Germany series: Systainer). All containers stacked together are 1.26 m high,

29.6 cm deep, and no wider than 49.6 cm. All containers are impact-resistant as well as dust- and splashwater-proof, to secure all parts of the olfactometer.

All parts are attached within the container system to ensure safety during transportation. In particular, the glass odor bottles are secured in a custom built mount.

Different airflow sources can be used for the pilot air and the odorized airflow of the olfactometer. In the MR setting, vector air is normally provided by the laboratory distribution network and can be obtained from a regular clinic air wall outlet, using a pressure regulator (range from 1.0 to 3.0 bar). Additionally, the olfactometer can also be used with a portable oil-free air compressor (e.g. fiac AIR COMPRESSORS, Italy series: DE 50/254) or a transportable gas container.

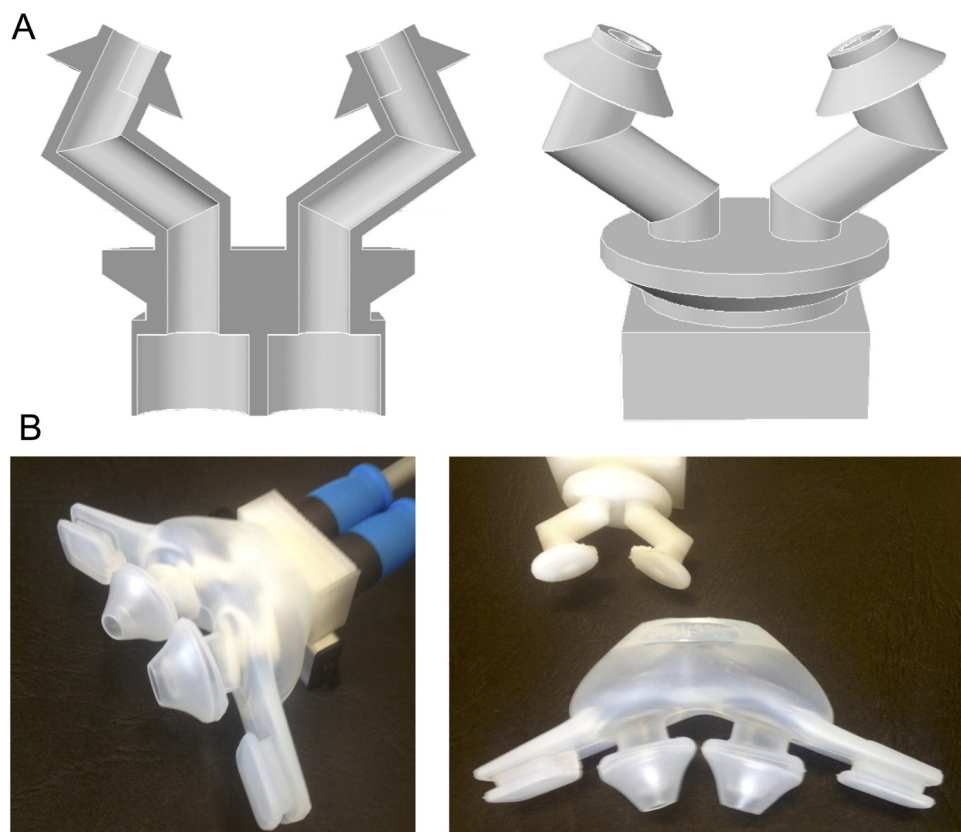


Fig. 3. Nasal mask and inlet. (A) Schematic illustration of the nosepiece, which can be used for bilateral or lateral presentation of odors (AutoCad drawing can be found in [supplementary materials](#)). (B) On the right side: the nasal mask with inlet and connection to the olfactometer and on the left side: the disassembled parts.

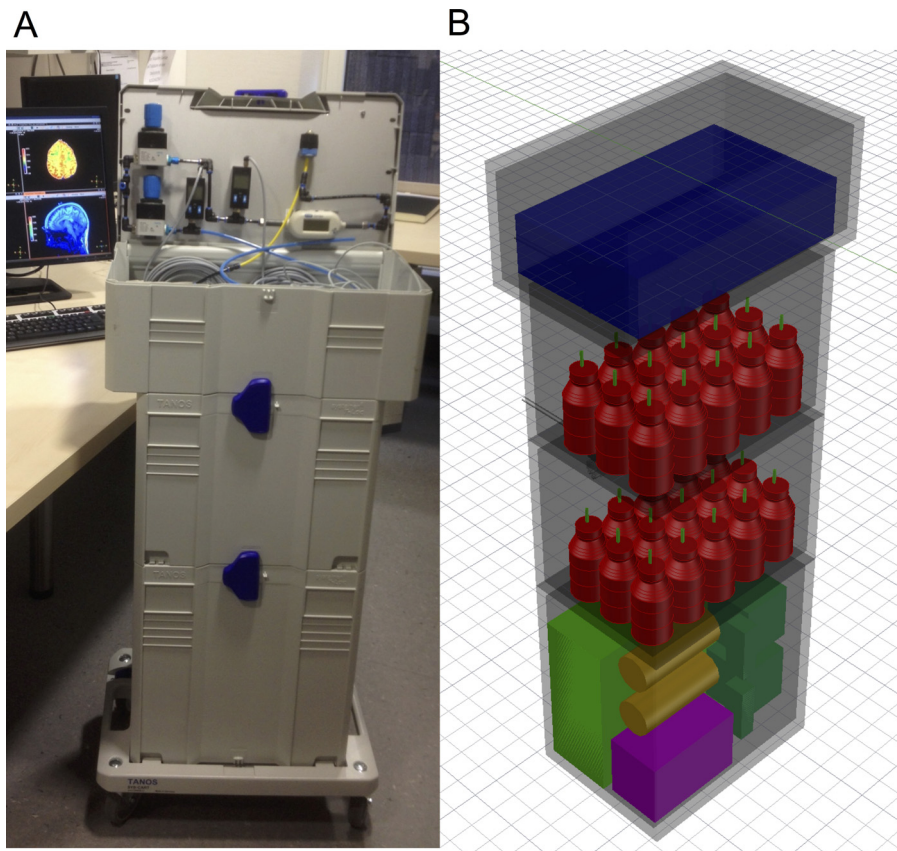


Fig. 4. The container system in the MR setting and a schematic Auto Cad drawing of the container system the olfactometer is built into.

2.3. Experimental designs

Experimental designs and upcoming research questions change frequently. Therefore, the olfactometer setup has to be flexible. This includes the control unit as well as the delivery unit.

The control unit mainly consists of an Arduino Mega 2560 microcontroller board, with 54 digital I/O pins and 16 analog inputs and a USB connection. The Arduino microcontroller controls the relay board that controls the valve terminals, which switch the control air and the odorized airflow. For the control unit Matlab (Matlab, R2014, MathWorks, Natick, US) is chosen as a software platform, because of the very precise temporal capabilities for controlling stimuli as well as capturing measurements such as reaction times and key-presses, and its operating-system-independent availability. In addition, the precise recording of temporal information is of high importance for the acquisition of trigger signals sent by the MR scanner that enables exact synchronization. Furthermore, very helpful toolboxes are provided for Matlab to realize psychological paradigms. For example the Psychtoolbox (<http://psychtoolbox.org>, Brainard, 1997) offers a free set of functions for vision and neuroscience research. We highly recommend Matlab to control the olfactometer, but it is also possible to control it by using Presentation software (Neurobehavioral Systems Inc.) as an interface. An extract of the Matlab code can be found in [supplementary materials](#), which displays the triggering of the relay board and the synchronization with an experiment.

Overall, the design enables a fast computer-controlled presentation of odorous stimuli in absence of auditory, tactile and thermal confounders. To help monitor proper operation during the experiment, LEDs of the relay boards signaling the state (closed-open) of the channels, are connected to plexiglas bars,

which make the states of the electric circuits visible from the outside (Fig. 5).

For the delivery unit the olfactometer design uses the method of pneumatically controlled plastic pinch valves that enable the use of separate independent channels for each odor. In combination with the modular design the possibility of expansion of additional channels, as well as measuring and control instruments has been implemented. Thus, the channels are easily and rapidly expandable to every necessary number of channels for the specific research question at hand. A higher number of channels support a higher number of repetitions within a condition without the need of presenting one odor multiple times.

Moreover, throughout the whole system push-in and click fittings (by FESTO, Germany from the Quick Star-series for fast connection and disconnection of tubes and from the NPKA-series for fast connection due to one-hand one-click operation completely made from plastic) are used. These fittings of the same size were used to facilitate and accelerate alterations of the olfactometer and to speed up the set-up time before testing.

3. Olfactometer: from air to odor

In this section the general construction of the olfactometer is described (Figs. 7 and 8). As written before, the olfactometer can be divided into two parts: control unit and delivery unit. In an MR setting, connections between these two parts pass through the waveguides (Fig. 6).

3.1. Control unit

The control unit, located within the control room of the MR setting contains all electrical and metal parts. It contains the air-supply

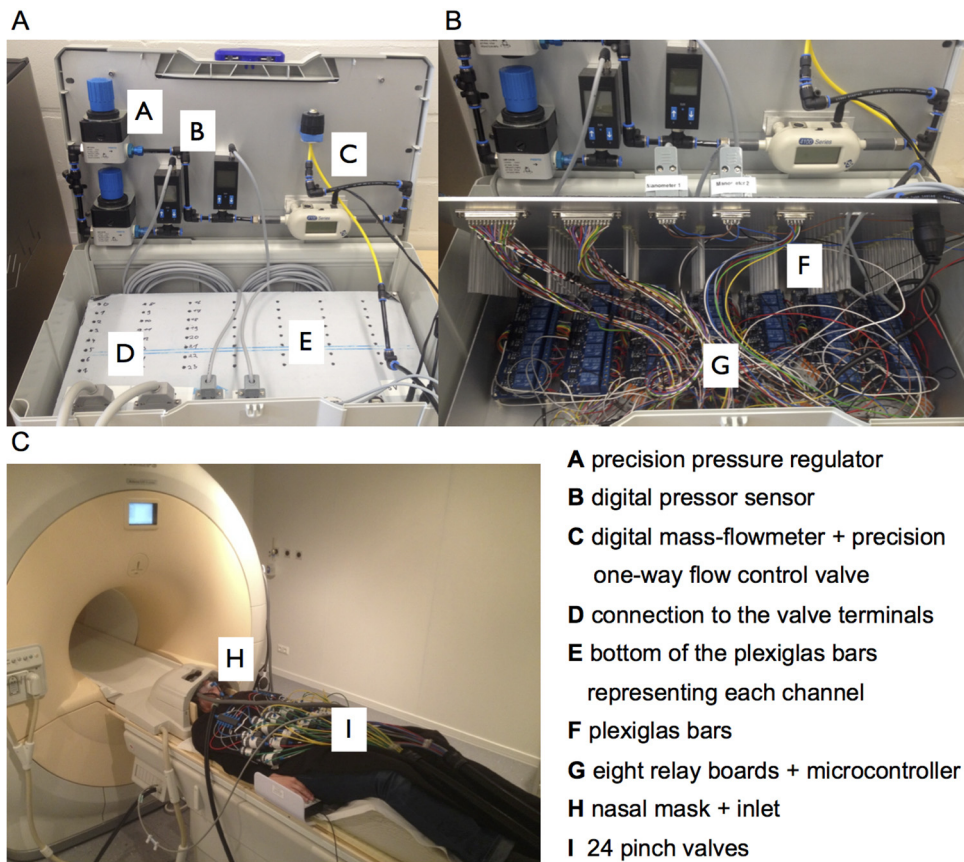


Fig. 5. Parts of the control unit and the delivery unit of the olfactometer. (A) The outside of the control unit box including two precision pressure regulators (one for the odor line and one for the pilot line), two digital pressure sensors (one for the odor line and one for the pilot line), a digital mass-flowmeter and a precision one-way flow control valve, to control airflow of the odor line. (B) The inside of the control unit box with eight relay boards and one microcontroller connected with jumper cable. LEDs of the relay boards are connected to plexiglas bars. (C) Part of the delivery unit and a participant in front of the MRI scanner.

(clinic air wall outlet, portable oil-free air compressor or transportable gas container), followed by reservoirs (combined with inlets of in-line HEPA filtration units) for compressed air, filled with activated charcoal, utilized as an air filter. After filtration, the air line is split into the odor line and the pilot line. Before reaching the valve terminals, both air lines pass a precision pressure regulator and a digital pressure sensor. The pressure regulator of the odor line is set to 1 bar and the pressure regulator of the pilot line is set to 3 bar. The odor line also includes a digital mass-flowmeter followed by a precision one-way flow control valve set to 1.5 l/min, to ensure constant flow rates throughout the experiment. Next both air lines pass a 24 channel miniature valve terminal comprising 24 2/2-way miniature valves (these valves block or open the odor lines up to the pinch valves) for the odor line and 24 3/2-way miniature valves (these valves block or open the pilot lines – when opened the air can escape through exhausts) for the pilot line. Both valve terminals are controlled via Matlab software and an Arduino Mega 2560 microcontroller board that is connected to six 8-channel relay boards (Fig. 5). By passing the valve terminal the odor line is split into 24 lines each passing a check valve before reaching the odor bottle to prevent contamination of the air lines by odorants (Fig. 8). When a channel is opened the yet odorless air is led through the liquid odorant (50 ml) within a gas washing odor bottle (Sezille et al., 2013). The now odorized air exits the bottle through a 12 m long tube leading to the delivery unit. The pilot line splits into 24 lines when passing the valve terminal and leads directly to the delivery unit through 12 m long tubes. All tubes leading to the delivery unit are clustered together into two tube-bundles each consisting of 12

tubes of the odor line, 12 tubes of the pilot line and one tube for exhaust ventilation. All tubes are made of polyethylene and thereby are food save and chemical and hydrolysis resistant. For exhaust ventilation a vacuum pump and an additional filter, as described above, are located within the control room. Each bundle is secured by protective tubing with an outer diameter of 42.5 mm and inner diameter of 36.5 mm.

3.2. Delivery unit

The connections between the control unit and the delivery unit (i.e. the control room and the MR testing room) pass through the waveguides. Each tube-bundle is passed through one wave guide. Each odor line passes through a separate pneumatically controlled plastic pinch valve, which is controlled via the pilot line. A valve is closed when pilot air is added and opens when pilot air is released. If an odor passes through the pneumatic valve it passes one of two distributors and leads to the nasal mask. Each distributor connects 12 odor channels and one exhaust ventilation channel with the nasal mask. With keeping the distance between pinch valves and nasal mask and the size of the distributors as small as possible a small dead volume of only 0.25 cm³ for each channel is achieved. Within the nasal mask a 3D printed inlet is placed, which enables the lateral distribution of an odor to either one of the nostrils or the bilateral application to both nostrils. This inlet also consists of a connection to the exhaust ventilation through the left and right cannulas to ensure an evacuation of odors from the nasal mask and thus to avoid cross contaminations.

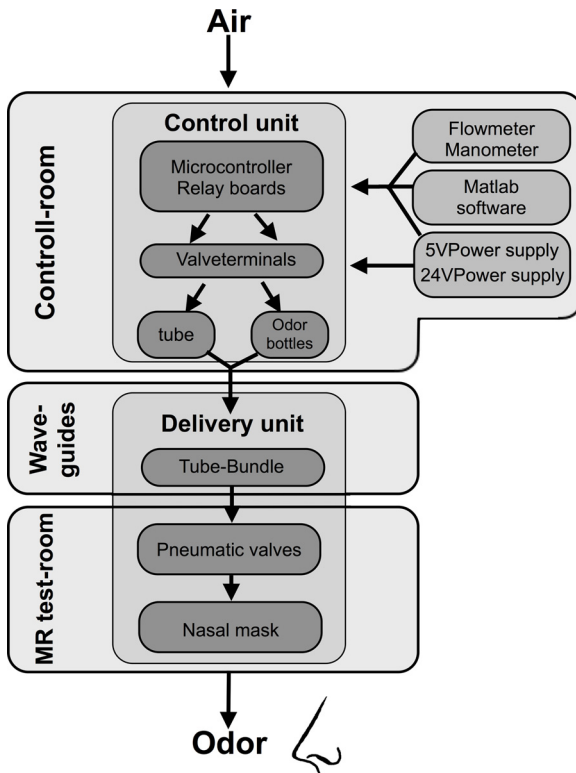


Fig. 6. Schematic course from air to odor through the olfactometer. The olfactometer can be divided into two parts: control unit and delivery unit. In an MR setting, these units are connected via two tube bundles, which are passed through the waveguides.

4. Experimental validation

In this section, results of an fMRI study and measurements of the real time chemical ionization mass spectrometer (CIMS, Airsense.net, MS4 GmbH, Germany) (for detailed information see Hornuss et al., 2007) will be reported to prove the functional performance of the olfactometer. The fMRI study is conducted to prove the ability of this olfactometer design to produce distinguishable neural activations between odorized and odorless air and between the emotional qualities of odors (pleasant vs. unpleasant).

In addition, with the mass spectrometer measurements the temporal resolution and concentration stability of odor presentation are analyzed.

4.1. fMRI study

The described olfactometer was used in an fMRI experiment with 17 neurologically healthy human subjects (8 male and 9 female; mean age: 22.5 years; range: 19–29; SD: 2.4). All participants were right-handed and had normal or corrected-to-normal vision. All subjects gave informed written consent after a detailed oral and written explanation of the procedures. The study received ethical approval by the Ruhr-University Bochum, which is in line with the Declaration of Helsinki.

4.1.1. Stimuli and task

An event-related design was used, comprising 12 odors that were presented. 6 negative and 6 positive odors from different categories like food, flower and body odors, chosen on the basis of previous work (Bestgen et al., 2015) were used as stimuli in this

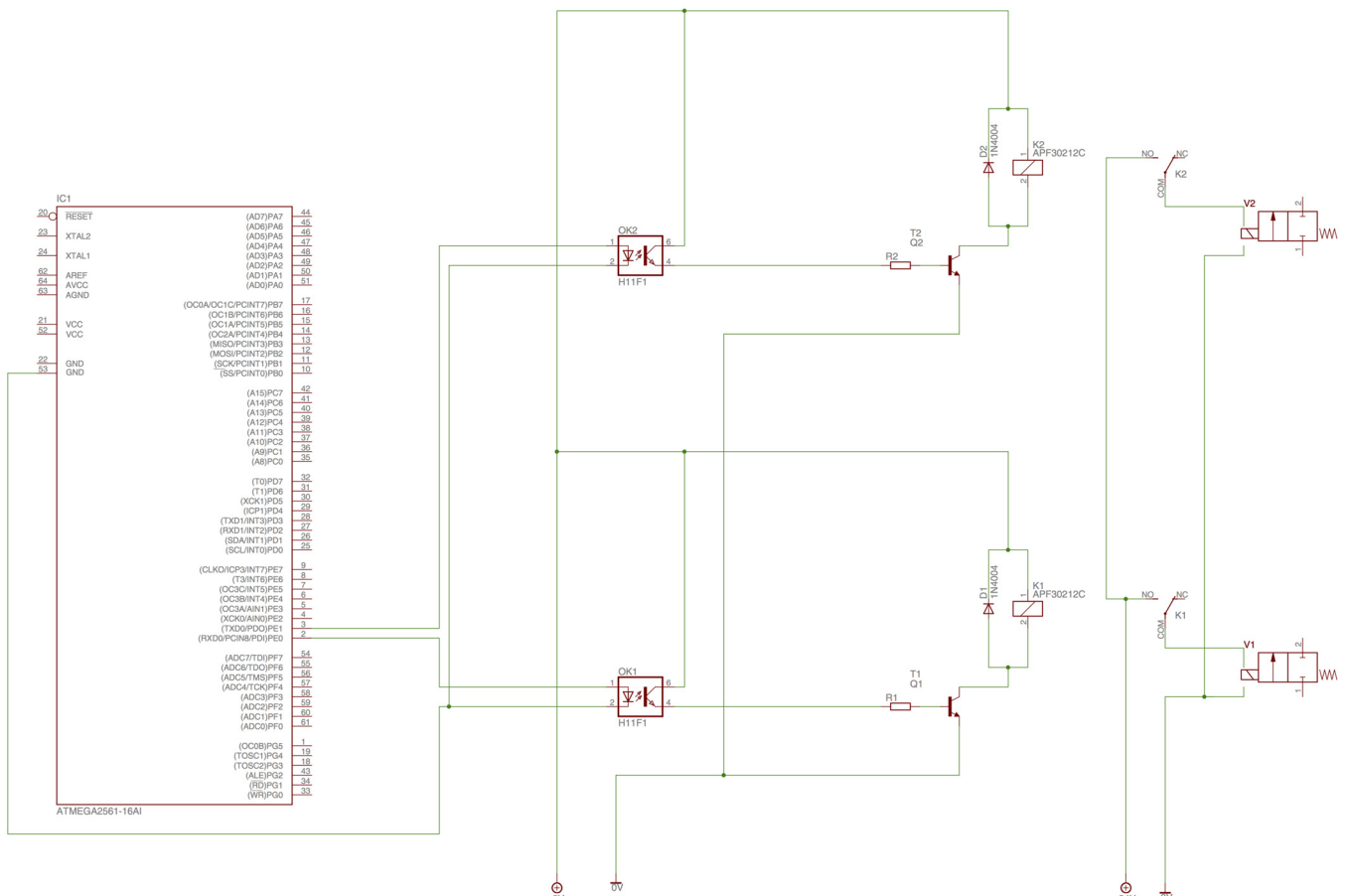


Fig. 7. Schematic illustration of the olfactometer electric circuits.

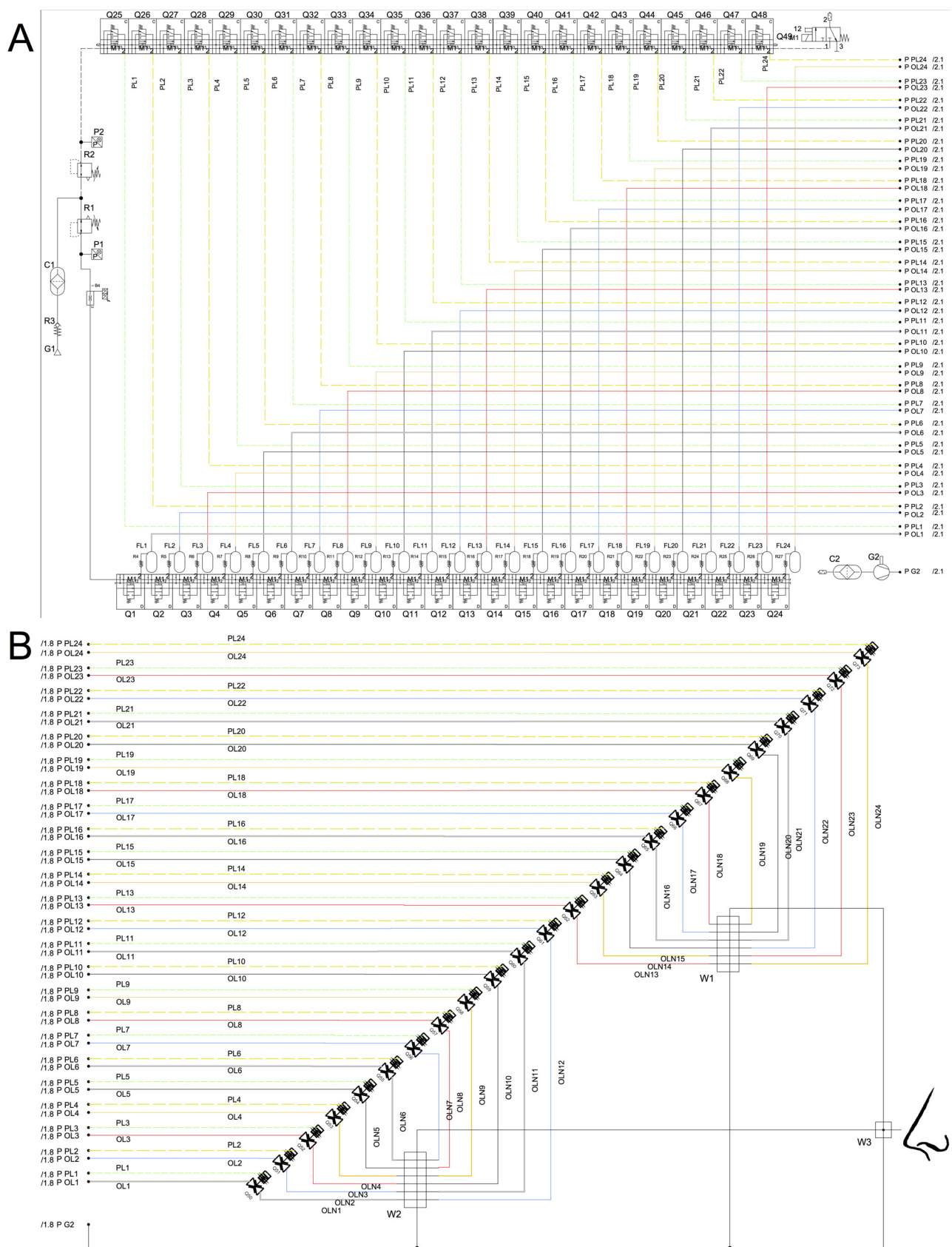


Fig. 8. Schematic illustration of the olfactometer pneumatic circuits. (A) Pneumatic circuits of the control unit. (B) pneumatic circuits of the delivery unit.

Table 1

Activation clusters resulting from the contrast odors > air at $p < .001$ (peak-level).

Cluster size	T-score	Cluster-level p-value (corr.)	MNI coordinates (x,y,z)			Anatomical structure
904	6.81	<.001	15	0	-14	Right amygdala
			32	3	-21	Right amygdala
			21	11	-15	Right piriform Cortex
322	6.66	<.001	-39	27	-17	Left inf. OFC
			-29	33	-14	Left inf. OFC
579	6.62	<.001	-30	0	-20	Left amygdala
			-20	-12	-18	Left hippocampus
			-20	-9	-11	Left hippocampus
			-41	5	-2	Left insula
303	5.59	<.001	-41	14	2	Left insula
			-35	21	-2	Left insula
			44	12	-5	Right insula
37	4.27	.003				

MNI coordinates, standard coordinates by the Montreal Neurological Institute; OFC, orbitofrontal cortex; inf., inferior.

experiment with ambient air as a neutral odor. The negative odors were: Garlic (Garlic oil blend), Sweat (Isovaleric acid), Raw meat (3-Acetyl-2,5-dimethylthiophenene), Onion (Onion oil, artificial), Feces (Skatole), and Vinegar (Acetic acid) and the positive odors were: Rose (Rose absolute, Moroccan), Lemon (Lemon oil), Caramel (Ethyl maltol), Grass (cis-3-Hexen-1-ol), Mint (*L*-Carvone, 99%) and Lavender (1-Octen-3-yl acetate). All odors were provided by Sigma

Aldrich, Germany (list of odors can be found in [supplementary materials](#)).

The participants had to perform a rating task with 54 trials divided into 3 blocks. In each trial the odor was presented for 4000 ms. Prior to this, the participants got a sniff cue for 1 s. Moreover, all participants were instructed to concentrate on an oral respiration through the whole experiment. Then a rating scale

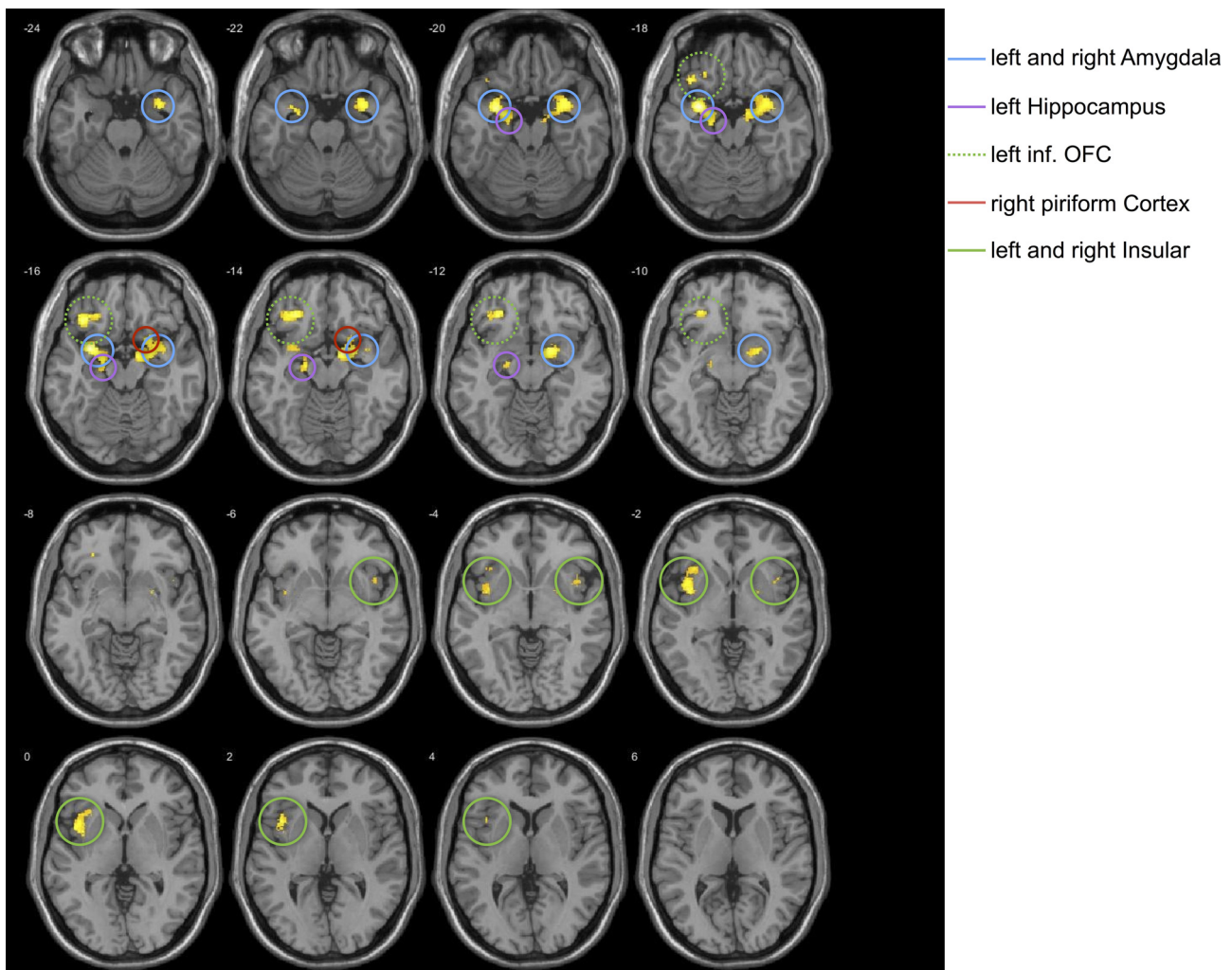


Fig. 9. Significant activation cluster for the contrast odor > air.

appeared for 4000 ms and the participant had to rate the pleasantness of the presented odor on a 6-point scale.

4.1.2. Set-up, statistics and imaging

The experiment was performed using a Philips 3T Achieva MR scanner with a 32 channel SENSE head coil. The olfactometer was setup in the scanner control room. The 12 m long tube, which connects the control unit and the delivery unit was passed through the waveguides from the side of the scanner and then connected to the control unit. The vector air was provided by the laboratory distribution network and obtained from a regular clinic air wall outlet with the use of a suitable pressure regulator.

A T1 weighted structural image was acquired for each participant at the beginning of the experimental session (220 slices, voxel size = 1 mm × 1 mm × 1 mm, TE = 3.8 ms, flip angle = 8°). T2* weighted EPIs were acquired in an ascending sequence of 30 slices (voxel size = 2 mm × 2 mm × 3 mm, TR = 2100 ms, TE = 30 ms).

The functional and structural images were pre-processed using the latest release of SPM8 (<http://www.fil.ion.ucl.ac.uk/spm/software/spm8>, revision number 6313). The preprocessing included slice time correction to the middle slice of each volume, realignment and unwarping, coregistration of the T1-weighted image to the mean T2*-weighted image, segmentation of the T1-weighted image and deformation to spatially normalize the images into a standard anatomical space (Montreal Neurologic Institute, MNI), and spatial smoothing using an isotropic 8 mm (full-width half-maximum) Gaussian kernel to account for intersubject differences, to reduce noise and to fulfill the assumptions for the use of GRF theory. Monte Carlo simulations (10,000 iterations) indicated that a cluster size of 37 or more voxels at $p < 0.001$ uncorrected would reduce false positives to a corrected level of $p < .05$ (a correction for multiple comparisons). Accordingly, at whole brain level, all clusters that passed this threshold are reported.

4.1.3. Results

To prove the functional performance of the olfactometer, two analyses were performed. In a first step, a *t*-test with the contrast odor versus air was conducted to reveal the overall functional capacity. Secondly, a *t*-test with the contrast unpleasant versus pleasant odors was conducted to show the qualitative transfer of odor quality. The *t*-test of odors versus air revealed 5 significant clusters, each consisting of multiple local maxima (Table 1). Stimulation with odorants lead to significantly increased BOLD signals in the bilateral amygdala, the bilateral insula, the left hippocampus, the left inferior orbitofrontal cortex (OFC) and the right piriform cortex (primary olfactory cortex, Fig. 9).

The contrast pleasant versus unpleasant odors yielded 6 significant clusters with multiple local maxima (Table 2).

Bilateral activation was present in the insula and the inferior orbitofrontal cortex (secondary olfactory cortex). Unilateral activations were found in the right piriform cortex, the right superior orbitofrontal cortex, the left amygdala and the left hippocampus (Fig. 10).

4.1.4. Discussion

Activations in the piriform cortex, the amygdala, the OFC, the hippocampus and the insula were found for odor processing. These areas represent the anatomical order of odor processing (Lundström et al., 2011). Main recipients of the axonal projections from the olfactory bulb are the piriform cortex and the closely located amygdala. Information from the piriform cortex and amygdala are relayed to OFC, hippocampus and in parallel the insula (Gottfried, 2010).

In addition, for the valence specific response higher activation of positive odors in contrast to unpleasant odors was found in the same areas found that are activated during odor processing. This points to valence specific processing of odor emotionality. In particular, activations in the left amygdala highlight the special anatomical feature of the olfactory system, the close connection of the olfactory processing regions and the emotion processing region (e.g., Herz, 2005), with the amygdala being the core brain region for emotion processing and emotional memory (Aggleton and Mishkin, 1986; Pessoa and Adolphs, 2010). Overall, these results reveal the functional efficiency of the new olfactometer-features adapted particularly for use in fMRI studies.

4.2. Chemical ionization mass spectrometer testing

The chemical ionization mass spectrometer (CIMS) is a highly sensitive method to test the concentration of the gas output over time. The method is based on an ion molecule reaction. The main components of the CIMS are a flowreactor, an ion source and a mass spectrometer for the ion detection. The gas of an odor of interest is integrated in an efficient ion molecular reaction which results into a count of particles with the specific molecular mass of the odorant of interest, thus allowing to measure the proportion of odor molecules present in a given airstream, for example parts per million (ppm). Here the CIMS is used to examine the responsiveness of the above introduced pneumatically controlled plastic pinch valves and the stability of odorant concentration over time. The CIMS is connected to the end of both cannulas of the nasal mask inlet (replacing the participants nose), thus measures represent responsiveness and stability of the hole system rather than single parts. Responsiveness can be seen as the latency to reach the plateau of odor concentration from the signal sent by the control unit to open the pneumatically controlled pinch valve, which are located directly in front of the participants' nose within the MR scanner. The results of the

Table 2

Activation clusters resulting from the contrast pleasant > unpleasant odors at $p < .001$ (peak-level).

Cluster size	T-score	Cluster-level <i>p</i> -value (corr.)	MNI coordinates (x,y,z)			Anatomical structure
100	7.64	<.001	23	12	-17	Right piriform Cortex
209	6.90	<.001	-29	-2	-17	Left amygdala
			-20	-9	-15	Left hippocampus
206	6.61	<.001	36	24	-3	Right insula
204	5.49	<.001	33	35	-12	Right inf. OFC
			21	30	-15	Right sup. OFC
151	5.32	<.001	-30	32	-14	Left inf. OFC
			-21	20	-17	Left inf. OFC
			-23	29	-17	Left inf. OFC
49	4.37	.001	-33	21	2	Left insula

MNI coordinates, standard coordinates by the Montreal Neurological Institute; OFC, orbitofrontal cortex; inf., inferior; sup., superior.

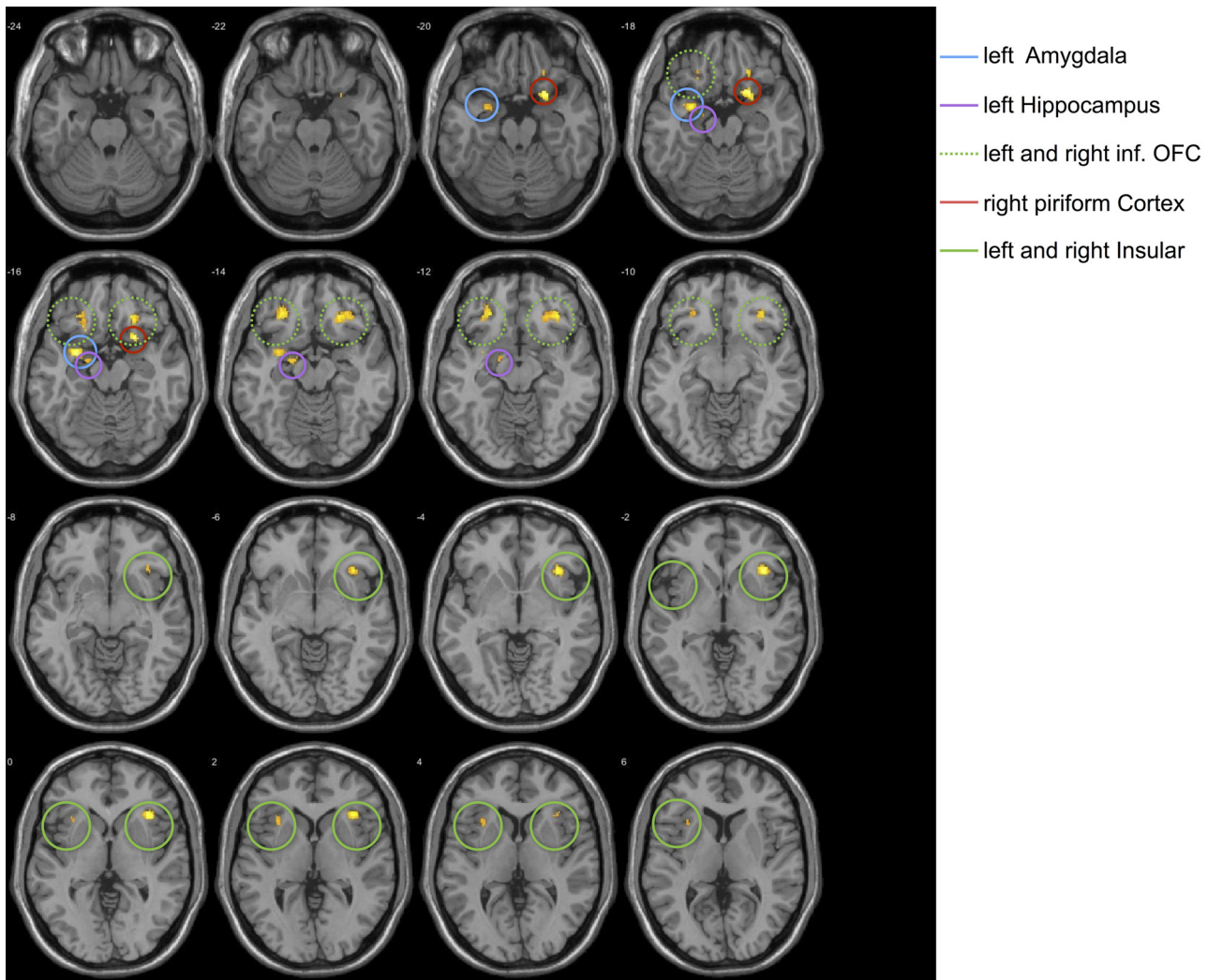


Fig. 10. Significant activation cluster for the contrast pleasant odors > unpleasant odors.

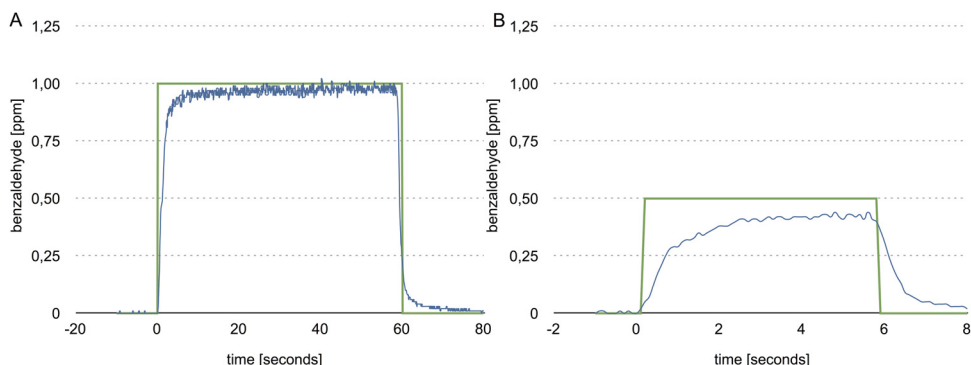


Fig. 11. Results of the chemical ionization mass spectrometer for (A) 1 min and for (B) 6 s. The upper lines represent the signal for opening and closing of the pinch valves. The other line represents the recorded concentration of benzaldehyde as a representative odor.

measurement of responsiveness show a latency of 350 ms, 600 ms and 1000 ms to reach 50%, 75% and 95% of the plateau concentration (Fig. 11). The stability of odor concentration is measured as the percentage of fluctuation around the plateau concentration over time, once the plateau is reached. The results show a stable concentration of .97 ppm ($SD = .01$) with fluctuation of less than 5% (4.9% peak-peak fluctuations/mean and 1.45% standard deviation/mean) over 1 min (Fig. 11).

5. Conclusion and limitations

Olfaction in contrast to other sensory systems is still a less studied sense using fMRI. Based on its specific characteristics like the close anatomical connection to the limbic system, with only two synapses between the olfactory neuron and the amygdala (Herz, 2005) and a minor involvement of the thalamus in contrast to other sensory modalities (although recently a greater contribution

of the medidorsal thalamic nucleus to olfaction is discussed, for review see [Courtial and Wilson, 2015](#)), the olfactory systems and the processes related to it gain more and more interest. Furthermore, olfactory deficits are known to be present in neurological diseases such as Alzheimer's and Parkinson's disease ([Doty et al., 2015; Landis et al., 2005](#)) and psychiatric disorders like Schizophrenia and post-traumatic stress disorder (PTSD, [Doty et al., 2015; Vasterling et al., 2000](#)) and therefore represent an important field of olfaction research. In addition to the development of the specific technical innovations of the olfactometer for use in fMRI studies, the olfactometer design is also adaptable to different research questions. Not only the number of channels (that directly represent the number of odors applicable) of the olfactometer can be reduced or extended, the control unit controllable with Matlab software package enables a large number of degrees of freedom to conduct different experiments with rapid on-off timing (block or event-related designs, including stimuli from other sensory systems).

The results of the pilot fMRI study support the functional efficiency of the olfactometer and show activation in brain regions that have frequently been mentioned in previous studies on olfactory perception. Activations of the right piriform cortex, the left inferior-OFC, left and right amygdala, left and right insula and left hippocampus have been found for the contrast odor versus air. These activations are in line with previous findings by [Gottfried et al. \(2002\)](#). Beyond these results, the contrast between positive and negative odors clearly point out that the olfactometer is able to deliver odor quality. A higher activation in the orbitofrontal gyrus, which has been associated with valence specific responses ([Anderson et al., 2003; Gottfried et al., 2002; Zald and Pardo, 1997](#)) is found for pleasant odors. Moreover, higher activations were found in the right piriform cortex, the left amygdala and the left hippocampus. These findings replicate previous findings by [Royet et al. \(2000, 2001\)](#) when participants had to evaluate odor valence and, thus, can verify the correct functioning of the olfactometer.

Additionally, the results of the CIMS measurement verify the temporal precision and stability of concentration of the described olfactometer. The described latency of 1000 ms to reach 95% is more than acceptable considering the low flow rates of only 1.5 l/min and the use of MR compatible pinch valves ([Lundström et al., 2010](#)). Because of the close dependency between the perception of an odor and its concentration, it is important to ensure a stable concentration over time, which is proven over a 1 min period. The temporal resolution and stability of concentration allow for consistent and comparable results between subjects. Moreover, in addition to the innovative features of this olfactometer design, it also provides an inexpensive alternative to the currently commercially-available olfactometers. A version of the MRI-compatible olfactometer with 24 channels will cost approximately 5900 Euro (Material-list can be found in [supplementary materials](#)). Given the results of the CIMS stable concentrations over time can be achieved. Nevertheless, with this olfactometer design only fixed concentrations can be used. It is not possible to dynamically change concentrations, but with the many of odor channels available it possible to apply the same odor in different concentrations using different channels, during an experiment. Furthermore, only odors in a liquid phase can be applied. The advantage here is that many odors can be dissolved in odorless liquids (e.g. using diluent propylene glycol). The olfactometer does not control and adapt airflow humidity and temperature. As already recommended by [Sezille et al. \(2013\)](#), these two parameters were left out of the design to remain simplicity of the olfactometer. In order to solve the temperature problem in a quick and unconventional way, mobile baby bottle warmer can be used. Without adjusting humidity or temperature, the airflow should be restricted to 5 l/min to avoid an exceedance of the pain threshold ([Loetsch et al., 1998](#)). This design does not take

respiratory recordings into account. These recordings should be considered to be synchronized with odor stimulation. Moreover, with this set-up an equally distributed airflow to the left and right exit of the nasal mask can be technically assured, but the influence of the asymmetrical internal nasal resistance should be considered (see [Eccles et al., 1989](#)). In conclusion, the olfactometer design presented in this paper can be seen as a realistic and feasible solution to overcome the challenges of presenting olfactory stimuli within the MR setting.

Appendix A. Supplementary data

Supplementary data associated with this article can be found, in the online version, at <http://dx.doi.org/10.1016/j.jneumeth.2015.12.009>.

References

- Aggleton J, Mishkin M. The amygdala, sensory gateway to the emotions. In: Kellermann H, editor. *Emotion: theory, research and experience: biological foundations of emotion*, vol. 3. Orlando, FL: Academic Press; 1986. p. 281–99.
- Anderson AK, Christoff K, Stappen I, Panitz D, Ghahremani DG, Glover G, et al. Dissociated neural representations of intensity and valence in human olfaction. *Nat Neurosci* 2003;6(2):196–202.
- Andrieu P, Bonnans V, Meneses J, Millot JL, Moulin T, Gharbi T. A modular, computer-controlled system for olfactory stimulation in the MRI environment. *Behav Res Methods* 2014;46(1):178–84. <http://dx.doi.org/10.3758/s13428-013-0362-x>.
- Bestgen A-K, Schulze P, Kuchinke L. Odor emotional quality predicts odor identification. *Chem Senses* 2015;40(7):517–23.
- Brainard DH. The psychophysics toolbox. *Spat Vis* 1997;10:443–6.
- Borromeo S, Hernandez-Tamames JA, Luna G, Machado F, Malpica N, Toledoano A. Objective assessment of olfactory function using functional magnetic resonance imaging (fMRI). *IEEE Trans Instrum Meas* 2010;59(10):2602–8.
- Cuevas I, Gérard B, Plaza P, Lerens E, Collignon O, Grandin C, et al. Development of a fully automated system for delivering odors in an MRI environment. *Behav Res Methods* 2010;42(4):1072–8.
- Courtial E, Wilson DA. The olfactory thalamus: unanswered questions about the role of the mediodorsal thalamic nucleus in olfaction. *Front Neural Circuits* 2015;9(49). <http://dx.doi.org/10.3389/fncir.2015.00049>.
- Doty R, Hawkes CH, Good KP, Duda JE. Odor perception and neuropathology in neurodegenerative diseases and schizophrenia. In: Doty RL, editor. *Handbook of olfaction and gustation*; 2015. p. 403–52.
- Eccles R, Jawad M, Morris S. Olfactory and trigeminal thresholds and nasal resistance to airflow. *Acta Otolaryngol (Stockh)* 1989;108:268–73.
- Gottfried JA. Central mechanisms of odour object perception. *Nat Rev Neurosci* 2010;11(9):628–41.
- Gottfried J, Deichmann R, Winston JS, Dolan RJ. Functional heterogeneity in human olfactory cortex: an event-related functional magnetic resonance imaging study. *J Neurosci* 2002;22(24):10819–28.
- Herz RS. Odor-associative learning and emotion: effects on perception and behavior. *Chem Senses* 2005;30(1):250–1. <http://dx.doi.org/10.1093/chemse/bjh209>.
- Hornuss C, Praun S, Villinger J, Dornauer A, Moehnle P, Dolch M, et al. Real-time monitoring of propofol in expired air in humans undergoing total intravenous anesthesia. *Anesthesiology* 2007;106:665–74.
- Kobal G, Hummel C. Cerebral chemosensory evoked potentials elicited by chemical stimulation of the human olfactory and respiratory nasal mucosa. *Electroencephalogr Clin Neurophysiol* 1988;71:241–50.
- Landis BN, Hummel T, Lacroix J-S. Basic and clinical aspects of olfaction. *Adv Tech Stand Neurosurg* 2005;30:69–105.
- Lorig TS, Elmés DG, Zaid DH, Pardo JV. A computer-controlled olfactometer for fMRI and electrophysiological studies of olfaction. *Behav Res Methods Instrum Comput* 1999;31(2):370–5.
- Loetsch J, Ahne G, Kunder J, Kobal G, Hummel T. Factors affecting pain intensity in a pain model based upon tonic intranasal stimulation in humans. *Inflamm Res* 1998;47:446–50.
- Lowen SB, Lukas SE. A low-cost, MR-compatible olfactometer. *Behav Res Methods* 2006;38(2):307–13.
- Lundström JN, Boesveldt S, Albrecht J. Central processing of the chemical senses: an overview. *ACS Chem Neurosci* 2011;2(1):5–16.
- Lundström JN, Gordon AR, Alden EC, Boesveldt S, Albrecht J. Methods for building an inexpensive computer-controlled olfactometer for temporally-precise experiments. *Int J Psychophysiol* 2010;78(2):179–89. <http://dx.doi.org/10.1016/j.ijpsycho.2010.07.007>.
- Pessoa L, Adolphs R. Emotion processing and the amygdala: from a 'low road' to 'many roads' of evaluating biological significance. *Nat Rev Neurosci* 2010;11(11):773–83.
- Popp R, Sommer M, Müller J, Hajak G. Olfactometry in fMRI studies: odor presentation using nasal continuous positive airway pressure. *Acta Neurobiol Exp (Warsz)* 2004;64:171–6.

- Royet JP, Zald D, Versace R, Costes N, Lavenne F, Koenig O, et al. **Emotional responses to pleasant and unpleasant olfactory, visual, and auditory stimuli: a positron emission tomography study.** *J Neurosci* 2000;20(20):7752–9.
- Royet JP, Hudry J, Zald DH, Godinot D, Grégoire MC, Lavenne F, et al. **Functional neuroanatomy of different olfactory judgments.** *Neuroimage* 2001;13(3):506–19.
- Sezille C, Messaoudi B, Bertrand A, Joussain P, Thévenet M, Bensafi M. A portable experimental apparatus for human olfactory fMRI experiments. *J Neurosci Methods* 2013;218(1):29–38, <http://dx.doi.org/10.1016/j.jneumeth.2013.04.021>.
- Sobel N, Prabhakaran V, Desmond JE, Glover GH, Sullivan EV, Gabrieli JDE. A method for functional magnetic resonance imaging of olfaction. *J Neurosci Methods* 1997;78(1–2):115–23, [http://dx.doi.org/10.1016/S0165-0270\(97\)00140-4](http://dx.doi.org/10.1016/S0165-0270(97)00140-4).
- Sommer JU, Maboshe W, Griebe M, Heiser C, Hörmann K, Stuck BA, et al. A mobile olfactometer for fMRI-studies. *J Neurosci Methods* 2012;209(1):189–94, <http://dx.doi.org/10.1016/j.jneumeth.2012.05.026>.
- Vasterling JJ, Constance JL, Hanna-Pladdy B. Head injury as a predictor of psychological outcome in combat veterans. *J Trauma Stress* 2000;13:441–51.
- Vigouroux M, Bertrand B, Farget V, Plailly J, Royet JP. A stimulation method using odors suitable for PET and fMRI studies with recording of physiological and behavioral signals. *J Neurosci Methods* 2005;142:35–44.
- Zald DH, Pardo JV. Emotion, olfaction, and the human amygdala: amygdala activation during aversive olfactory stimulation. *Proc Natl Acad Sci U S A* 1997;94(8):4119–24.